

ficient for the viability of the ILT model in the face of a large value of $\lambda_{\perp}(0)$.

With the above analysis in mind, let us consider the consequences of relaxing condition (4). The argument leading to Eq. 5 now fails because it may be possible to put in a much larger than average value of $\Delta\phi_i$ across links for which $T_{\perp}(\xi)$ is negative, thereby actually decreasing $\langle T_{\perp} \rangle$ by itself. However, consider a set of N links with an average value of $T_{\perp}(\xi)$ equal to $-\varepsilon(T)$; then an (not entirely trivial) argument analogous to that of the preceding paragraph shows that for such a configuration to give an energy advantage, we must have $N \geq \kappa/\varepsilon$ (or κ/ε^2 for $\varepsilon \leq 1$). Bearing in mind that by definition $\varepsilon \leq 1$ and that we have estimated $\kappa \sim 50$, we now ask if it is possible to find a distribution $f(t)$ of the $T_{\perp}(\xi)$ —even a pathological one—such that the probability of such an occurrence is, as a minimum, comparable to the inverse of the number of planes ($\sim 10^{-7}$, say). I have so far failed to find such a distribution and, although I have at present no rigorous proof, strongly suspect that none exists. Thus, although relaxation of condition (4) at first appears to prevent the derivation of a rigorous inequality such as Eq. 5, it should not affect the qualitative conclusions reached above.

The conclusion is that although a value of $\lambda_{\perp}(0)$ for TI-2201 greater than $10 \mu\text{m}$ would not definitively refute a generic form of the ILT model, it would as a minimum either violate one or more of assumptions (1) through (3) or constrain the ground state to have extremely large fluctuations in T_{\perp} (which should, at least in principle, be detectable in angle-resolved photoelectron spectroscopy measurements on a - or b -axis-oriented films). It remains to be seen whether a concrete version of the model having this feature can be constructed and shown to be physically reasonable.

REFERENCES AND NOTES

1. J. Wheatley, T. Hsu, P. W. Anderson, *Nature* **333**, 121 (1988).
2. P. W. Anderson, *Physica C* **185**, 11 (1991); *Phys. Rev. Lett.* **67**, 660 (1991); *Science* **256**, 1526 (1992).
3. S. Chakravarty, A. Sudbø, P. W. Anderson, S. Strong, *Science* **261**, 337 (1993).
4. P. W. Anderson, *ibid.* **268**, 1154 (1995).
5. B. D. Josephson, *Phys. Lett.* **1**, 241 (1962).
6. V. Ambegaokar and A. Baratoff, *Phys. Rev. Lett.* **10**, 49 (1963); erratum, *ibid.* **11**, 104 (1963).
7. D. van der Marel, J. Schützmann, H. S. Somal, J. W. van der Eb, *Proceedings of the 10th Anniversary Workshop on Physics, Materials and Applications*, Houston, March 1996 (World Scientific, Rivers Edge, NJ, in press).
8. The reader might reasonably ask why we should not simply use equation 1 of (72) and use the experimental ac conductivity to evaluate the second term. Although this is in principle possible, in practice any analysis in the cuprate superconductors that relies on finite-frequency effects is fraught with notorious difficulties. The advantage of the present analysis is that it relies only on properties of the ground state [note that there is no reason why $\lambda_{\perp}(0)$ itself should not be measured by a dc technique].
9. The function $T_{\perp}(\xi)$ cannot be positive definite for all ξ because of the requirement of Fermi antisymmetry. Assumption (4) is in effect the statement that the antisymmetry is completely satisfied by the in-plane behavior, and it turns out not to be satisfied by some familiar models, for example, a weakly paired 3D Fermi liquid with a tight-binding normal-state spectrum in the c direction; note however that it is satisfied by, for example, the standard LD model, provided that the matrix element t_{\perp} is constant across the ab plane.
10. It may be objected that (the analog of) Eq. 5 is spectacularly violated for the standard [Ambegaokar-Baratoff (6)] model of a single Josephson junction (which at first sight corresponds to the special case of the above calculation for $n = 2$) because it is a standard result that the Josephson coupling energy (the "superfluid density" up to a factor) is a small fraction of the total tunneling energy, whereas the quantity α is of order unity. However, to analyze this model along the above lines, one must consider the junction itself as being in series with whatever mechanism is responsible for "dephasing" the electrons in the bulk superconductors, as well as the effect of (non)conservation of the transverse momentum. Thus, it is not (or at least not obviously) a counterexample to the theorem (3).
11. Because I have been unable to locate a local-density approximation or similar calculation of t_{\perp} for TI-2201 in the literature, I estimate it at 0.02 eV.
12. B. S. Shastry and B. Sutherland, *Phys. Lett.* **65**, 243 (1990).
13. This work was supported by the NSF Science and Technology Center for High Temperature Superconductivity through grant NSF-DMR-91-20000 to the University of Illinois. I acknowledge helpful discussions and correspondence with D. Bonn, L. Cooper, J. Loram, R. J. Radtke, S. Sachdev, M. Salamon, F. Zuo, and, in particular, D. Loss and D. van der Marel; I also thank the last-named for permission to quote the results of (7) in advance of its publication. Finally, I am grateful to R. Martin for a critical reading of the manuscript.

14 May 1996; accepted 30 August 1996

Evidence for Charge-Flux Duality near the Quantum Hall Liquid-to-Insulator Transition

D. Shahar, D. C. Tsui, M. Shayegan, E. Shimshoni,*
S. L. Sondhi†

A remarkable symmetry has been observed between the diagonal, nonlinear, current-voltage (I - V_{xx}) characteristics taken in the fractional quantum Hall effect (FQHE) liquid state of the two-dimensional electron system and those taken in the bordering insulating phase. When properly selected, the I - V_{xx} traces in the FQHE regime are identical, within experimental errors, to V_{xx} - I traces in the insulator, that is, with the roles of the currents and voltages exchanged. These results can be interpreted as evidence for the existence of charge-flux duality symmetry in the system.

The theoretical understanding of the quantum Hall effect (QHE) is believed to involve the physics of the ideal states and that of localization. A precise theoretical account of the QHE phenomena is, not surprisingly, controversial, for it requires solving a problem with interactions, fractional statistics, and disorder—a rather formidable task. Nevertheless, considerable theoretical progress had been made in recent years in understanding the phase diagram of QH states and the transitions between them.

In a recent theoretical paper, Kivelson, Lee, and Zhang (1) used a flux attachment (Chern-Simons) transformation (2) to map

the two-dimensional electron system (2DES) at high magnetic field (B) onto a bosonic system under a different field B_{eff} . The advantage of this mapping is clear if one considers the "magic" Landau-level filling fractions (ν values) where the fractional quantum Hall effect (FQHE) liquid states are observed. At these ν values the Chern-Simons gauge field cancels, on average, the externally applied B , and the composite bosons (CBs) experience a vanishing B_{eff} . The incompressible FQHE states then arise as a result of the formation of a Bose-condensed, superconducting state of the CBs.

At ν values other than the magic ν values, the cancellation of the external B is not exact and, according to the bosonic picture, vortices are created in the CB condensate. For small deviations from magic ν values, the vortex density is small, and the vortices are localized by disorder and do not contribute to the long-wavelength electrical response. When the deviation from the magic ν values becomes sufficiently large, the superconductivity of the CBs is destroyed by the excess magnetic field and the

D. Shahar, D. C. Tsui, M. Shayegan, Department of Electrical Engineering, Princeton University, Princeton, NJ 08544, USA.

E. Shimshoni, Department of Physics and the Beckman Institute, University of Illinois at Urbana-Champaign, Urbana, IL 61801, USA.

S. L. Sondhi, Department of Physics, University of Illinois at Urbana-Champaign, Urbana, IL 61801, USA.

*Present address: Department of Mathematics-Physics, Oraniv, Tivon 36006, Israel.

†Present address: Department of Physics, Princeton University, Princeton, NJ 08540-0708, USA.

system becomes insulating. This results in a transition to an insulating phase or to a different QH state. Utilizing this bosonic formulation, Kivelson *et al.* proposed a set of approximate "correspondence rules" that relate the different QH states and allows construction of a phase diagram for the QH system in the disorder— B field plane (1). This set of rules implies that all continuous phase transitions between QH states and between QH states and insulators are in the same universality class when described in terms of the CBs.

We report here the results of a set of measurements that may shed additional light on the interplay between different phases of 2DES at high B . We have studied both the longitudinal (V_{xx}) and Hall (V_{xy}) current-voltage (I - V) characteristics near the QH liquid-to-insulator transition and found that (i) the I - V_{xx} curves exhibit a distinctive reflection symmetry between certain traces in the QH state and in the insulating phase in the range of B field where they are strongly nonlinear and B -dependent and (ii) at the same B and I values, the I - V_{xy} curves are nearly linear and virtually B -independent. Taken together, these observations may suggest the possibility that the system exhibits a form of charge-flux or electric-magnetic duality (3). We will elaborate on this possibility below.

We studied a high-mobility ($\mu = 5.5 \times 10^5 \text{ cm}^2 \text{ V}^{-1} \text{ s}^{-1}$), low-density ($n = 6.5 \times 10^{10} \text{ cm}^{-2}$) GaAs/Al_xGa_{1-x}As heterostructure grown by molecular beam epitaxy. A typical B trace of the diagonal resistivity ρ_{xx} for this sample is plotted in Fig. 1A. Attesting to the high quality of this sample is the set of FQHE states that includes the $\nu = 4/3, 2/3, 3/5, 2/5,$ and $1/3$ states, which are manifested as minima in the ρ_{xx} trace. The QHE series terminates at high B with a transition to an insulating (INS) phase. The transition point, B_c , is identified (4) with the common crossing point of the B field traces of ρ_{xx} taken at several temperatures T between 26 and 88 mK (see Fig. 1B). A systematic study of this transition was presented in (4).

In Fig. 2A we replot a selected set of I - V_{xx} traces, some of which were reported in (4). They were obtained from our sample at $T = 21 \text{ mK}$, at various B values in the vicinity of B_c . As mentioned in (4), with the exception of the trace taken closest to B_c , the I - V_{xx} curves are markedly nonlinear both in the $\nu = 1/3$ FQHE regime (short-dashed lines) and in the insulating phase (solid lines). Deep in the $\nu = 1/3$ FQHE regime ($B = 8.5 \text{ T}$), strong superlinear behavior is observed that is typical of a dissipationless QHE state. As we approach B_c , this superlinearity becomes less pronounced, and the curve taken closest to B_c

(long-dashed line) appears linear over the entire voltage range, within experimental error. At higher B , as we enter the insulating phase, the I - V_{xx} curves (solid lines) change in nature and are now sublinear, reflecting the insulating character of the conduction process. This sublinearity increases as we go deeper into the insulating phase. In Fig. 2, we have normalized the I and V units such that the dashed line, which is the I - V_{xx} curve closest to B_c , has unit slope. This amounts to defining the resistivity units in terms of the critical resistivity at the transition point, which was shown to be close to h/e^2 (4), where h is Planck's constant and e is the electron charge. For this measurement it is 23 kilohms.

A striking feature of the I - V_{xx} curves presented in Fig. 2A is their apparent reflection symmetry about the linear I - V_{xx} curve taken at B_c . To illustrate this symmetry we plot, in Fig. 2B, the same I - V curves as in Fig. 2A but with the I and V coordinates of the curves taken in the FQHE regime exchanged. The overlap between some pairs of traces is remarkable, with only small deviations that are not systematic in their direction or magnitude, or in their dependence on the distance from B_c . Such deviations are reasonable considering the inevitable presence of sample imperfections and slight inhomogeneities (5). The matching is maintained rather far from the tran-

sition point, over a range of 1.6 T. Similar symmetry is observed also for lower mobility samples, where the transition to the insulator is from the $\nu = 1$ QHE state, but over a rather narrower range in B of 0.1 T.

On a purely phenomenological level, the correspondence of the I - V_{xx} traces on both sides of the transition indicates that at least some of the special correlations that are responsible for the FQHE state survive the transition to the insulating phase. In other words, there exists a relation between the physical mechanism responsible for the nonlinear I - V_{xx} at a given B in the FQHE liquid regime and that at a corresponding B value in the insulating phase. This empirical statement can be made without any knowledge of the nature of this mechanism (6).

In order to investigate the nature of this correspondence, it is necessary to identify whether a systematic relation exists between the B values of the matched pairs of I - V_{xx} traces in Fig. 2B. In Fig. 3, we summarize the ΔB ($|B - B_c|$, Fig. 3A) and $\Delta \nu$ ($|\nu - \nu_c|$, Fig. 3B) values for each one of the I - V_{xx} traces in Fig. 2. The abscissa of the graphs of Fig. 3 designates the pairs, which are identified by a number in Fig. 2B, with smaller numbers denoting pairs that are closer to the transition. Solid circles designate I - V_{xx} characteristics taken in the $1/3$ FQHE state, and empty circles designate those taken in the insulator. Evidently, the

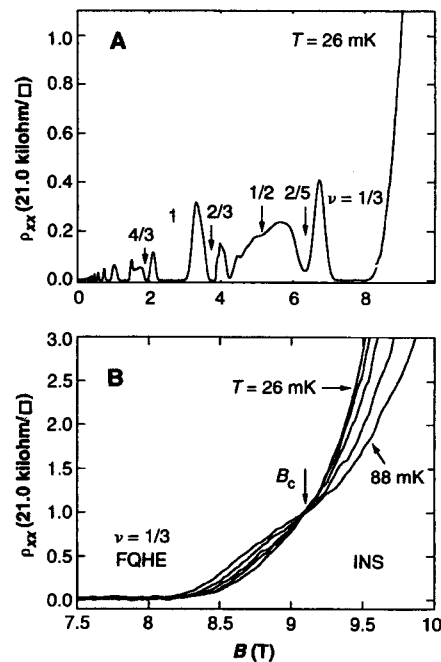


Fig. 1. (A) A typical B trace of ρ_{xx} for our sample. (B) The transition region near $B_c = 9.1 \text{ T}$. The temperatures for the traces are 26, 36, 48, 65, and 88 mK. The resistivities are in kilohms per square (that is, corrected for the geometry of the square bounded by the four-point probe).

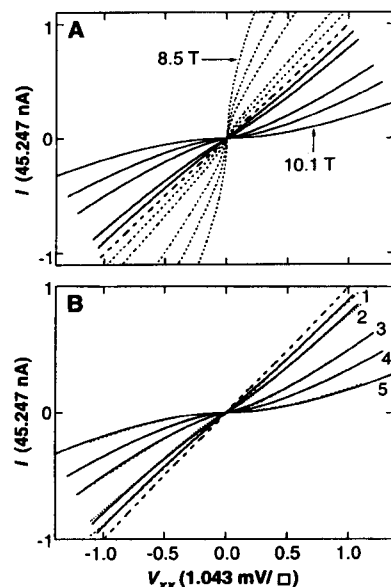


Fig. 2. (A) Plot of I versus V_{xx} at several values of B near B_c ; $T = 21 \text{ mK}$. Solid lines are in the insulating phase, and dotted lines are in the $\nu = 1/3$ FQHE liquid. The B values are 8.5, 8.6, 8.7, 8.9, 9, 9.1 (dashed line), 9.2, 9.3, 9.6, 9.8, and 10.1 T. (B) The same data as in (A) but with the I and V_{xx} coordinates of the traces in the $\nu = 1/3$ FQHE state (dotted lines) exchanged. The numbers are used to identify the pairs.

matched pairs are neither the same ΔB from the transition, nor the same $\Delta\nu$.

A clue to the correspondence is the interpretation of the reflection symmetry as the exchange of the I and V roles across the transition. Such an exchange is suggestive of the framework of charge-flux duality for 2D bosons (3). Here we consider a modified version (7) that has also been used (1, 8) in discussions of QH phase transitions. In the CB picture, the state at a generic ν contains both CBs and vortices: in the QH phase the CBs superconduct and the vortices are localized, whereas in the insulator the vortices superconduct and the CBs are localized. Hence, the natural candidate for the dual state to a filling factor with a certain ratio of the number of CBs (N_b) and vortices (N_v), N_b/N_v , is the filling factor with the inverse ratio, N_v/N_b .

In the vicinity of the $\nu = 1/3$ to insulator transition, the CBs "carry" three quanta of flux and hence, at filling ν , the state of a system with $N_b = N$ CBs has $N_v = N(\nu^{-1} - 3)$ vortices. It follows from this that its dual filling is $\nu_d = (1 - 3\nu)/[\nu + 3(1 - 3\nu)]$. A different way to express this, which also makes contact with the composite fermion (CF) description (9), is by introducing an auxiliary filling, $\nu' = \nu/(1 - 2\nu)$, that relates the electron filling factor ν to

that of the CF. Then, the dual fillings of the CBs are related by these auxiliary fillings as $\nu' = \nu'_c + \Delta\nu'$ and $\nu'_d = \nu'_c - \Delta\nu'$. In other words, dual filling factors for CBs are the same as particle-hole symmetric filling factors for CFs. The correspondence in terms of these auxiliary fillings (Fig. 3C) describes the matching significantly better than the attempts presented in Fig. 3, A and B. This result supports the notion that the I - V_{xx} matching reflects a symmetry of the underlying composite particles.

Thus far, we have introduced the notion of duality to summarize the experimental observation that I and the longitudinal V appear to trade places at ν values where, in the CB description, the numbers of CBs and vortices trade places. However, exchanging the numbers of CBs and vortices is not sufficient to ensure that the two states will be symmetric (10). The observed symmetry then implies that the dynamics of the CBs and vortices are also symmetric or, in the CF language, the system exhibits particle-hole symmetry. This is rather surprising because one cannot, a priori, assume a relation between the physics of the $1/3$ FQHE liquid and that of the insulator.

An additional conjecture, which we have tested experimentally, can be made by inspecting, in the CB picture, the possible implications of the I - V_{xx} symmetry on a measurement of the Hall voltage response in the transition region. Because the CB framework has only been applied so far to the linear response regime, we focus temporarily on the CB resistivity tensor (1), which is defined by the decomposition

$$\rho_c = \rho_b + \rho_{cs} \quad (1)$$

where ρ_c is the resistivity tensor measured in experiment, ρ_b is the CB resistivity tensor, and ρ_{cs} is the Chern-Simons term, which corrects ρ_b for the fact that the CBs carry flux that produces a purely Hall response through a "Faraday effect." For the $\nu = 1/3$ FQHE-to-insulator transition studied in this work, Eq. 1 can be written explicitly ($h/e^2 = 1$):

$$\begin{pmatrix} \rho_{xx} & \rho_{xy} \\ -\rho_{xy} & \rho_{xx} \end{pmatrix} = \begin{pmatrix} \rho_{xx}^b & \rho_{xy}^b \\ -\rho_{xy}^b & \rho_{xx}^b \end{pmatrix} + \begin{pmatrix} 0 & 3 \\ -3 & 0 \end{pmatrix} \quad (2)$$

Duality symmetry for the CBs implies that $\rho_b(\nu) = \rho_v^\dagger(\nu_d)$, where ρ_v is the resistivity tensor of the vortices. Also, currents and voltages for the bosons and vortices are related by the Josephson relation, that is, $\rho_v(\nu) = \sigma_b(\nu)$. Together these imply

$$\rho_b(\nu) = \sigma_b^\dagger(\nu_d) \quad (3)$$

Now, the observed symmetry between ν and ν_d under exchange of I and V can (in the ohmic regime) be expressed as:

$$\rho_{xx}(\nu) = 1/\rho_{xx}(\nu_d) \quad (4)$$

The only way to reconcile Eqs. 2, 3, and 4 is if $\rho_{xx}^b(\nu) = 1/\rho_{xx}^b(\nu_d)$ and $\rho_{xy}^b = 0$ everywhere in the vicinity of the transition, including the insulating side. This result implies that the measured ρ_{xy} is constant ($=3h/e^2$) everywhere in the transition region (11), indicating that ρ_{xy} is insensitive to whether the conduction process is that of a FQHE liquid or an insulator, and only cares about the "flux" attached to the CBs. Extending this line of argument to the nonohmic response regime, it follows that the Hall voltage would be linear with driving current even when the longitudinal V is distinctly not so.

To test these predictions we plot in Fig. 4 V_{xy} versus I traces taken at $T = 21$ mK and at B intervals of 0.1 T starting in the $\nu = 1/3$ FQHE phase ($B = 8.7$ T) and ending in the insulating phase ($B = 9.7$ T). In contrast to the longitudinal I versus V traces taken in the same T and the same B range (to compare, we replot in Fig. 4 the I - V_{xx} traces taken at $B = 8.7$ and 9.7 T). These curves are virtually B -independent and are close to linear with only minor deviations from a slope of $3h/e^2$ (12), in support of the predictions arising from the CB approach.

REFERENCES AND NOTES

1. S. A. Kivelson, D. H. Lee, S. C. Zhang, *Phys. Rev. B* **46**, 2223 (1992).
2. S. C. Zhang, T. H. Hansson, S. A. Kivelson, *Phys. Rev. Lett.* **62**, 82 (1989).
3. M. P. A. Fisher and D. H. Lee, *Phys. Rev. B* **39**, 2756 (1989). The many uses of duality transformations in statistical mechanics are reviewed in R. Savit, *Rev. Mod. Phys.* **52**, 453 (1980).
4. D. Shahar, D. C. Tsui, M. Shayegan, R. N. Bhatt, J. E. Cunningham, *Phys. Rev. Lett.* **74**, 4511 (1995).
5. We are currently studying the low-current region of the I - V values. Initial results show that, indeed, the symmetry ($\rho_{xx} \rightarrow 1/\rho_{xx}$) holds even at the "ohmic" regime.
6. In the absence of a microscopic model describing the conductivity process near the transition, the physical origin of the nonlinear I - V_{xx} traces is not clear. However, two comments are in order. First, as the dissipation mechanisms in the FQHE and insulating phases are distinctly asymmetric (in the former the dissipation is mainly in the contacts, whereas in the latter it is mostly in the bulk), an interpretation of

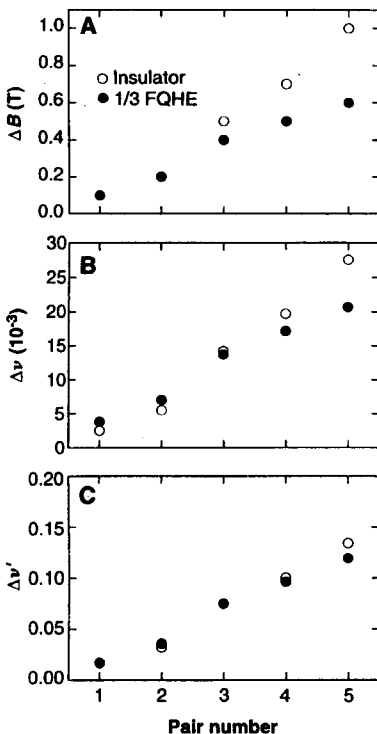


Fig. 3. Plots of (A) $\Delta B = B - B_c$, (B) $\Delta\nu = \nu - \nu_c$, and (C) $\Delta\nu' = \nu' - \nu'_c$ (see text) for each pair of matched I - V_{xx} traces in Fig. 2B versus the pair number. Pairs with smaller numbers are closer to the transition.

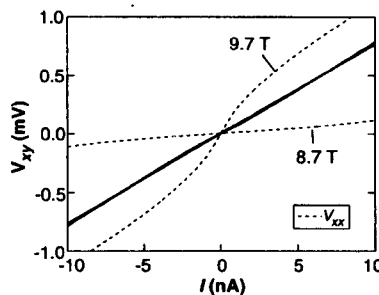


Fig. 4. Plots of V_{xy} versus I near the transition, taken at 0.1-T steps in the B range from 8.7 to 9.7 T. Dashed traces are of V_{xx} $T = 21$ mK.

- our symmetric, nonlinear $I-V_{xx}$ traces in terms of a simple Joule heating model is unlikely. Second, critical fluctuations are generally expected to lead to universal nonlinearities in the response. See, for example, N. Goldenfeld, *Lectures on Phase Transitions and the Renormalization Group* (Addison-Wesley, Reading, MA, 1992).
7. D. H. Lee and M. P. A. Fisher, *Phys. Rev. Lett.* **63**, 903 (1989).
 8. M. P. A. Fisher, *ibid.* **65**, 923 (1990); C. A. Lütken and G. G. Ross, *Phys. Rev. B* **48**, 2500 (1993).
 9. J. K. Jain, *Phys. Rev. Lett.* **63**, 199 (1989).

10. E. Shimshoni, S. L. Sondhi, D. Shahar, in preparation.
11. A. M. Dykne and I. M. Ruzin, *Phys. Rev. B* **50**, 2369 (1994); I. M. Ruzin and S. Feng, *Phys. Rev. Lett.* **74**, 154 (1995).
12. D. Shahar *et al.*, in preparation.
13. We thank L. W. Engel, M. P. A. Fisher, S. M. Girvin, S. A. Kivelson, and M. Stone for instructive discussions. Supported by the National Science Foundation and the Beckman Foundation.

13 June 1996; accepted 3 September 1996

Seismic Evidence for a Low-Velocity Zone in the Upper Crust Beneath Mount Vesuvius

A. Zollo, P. Gasparini, J. Virieux, H. le Meur, G. de Natale, G. Biella, E. Boschi, P. Capuano, R. de Franco, P. dell'Aversana, R. de Matteis, I. Guerra, G. Iannaccone, L. Mirabile, G. Vilardo

A two-dimensional active seismic experiment was performed on Mount Vesuvius: Explosive charges were set off at three sites, and the seismic signal along a dense line of 82 seismometers was recorded. A high-velocity basement, formed by Mesozoic carbonates, was identified 2 to 3 kilometers beneath the volcano. A slower (P -wave velocity $V_p = 3.4$ to 3.8 kilometers per second) and shallower high-velocity zone underlies the central part of the volcano. Large-amplitude late arrivals with a dominant horizontal wave motion and low-frequency content were identified as a P to S phase converted at a depth of about 10 kilometers at the top of a low-velocity zone ($V_p < 3$ kilometers per second), which might represent a melting zone.

In 1994 a seismic tomography study of the structure and magmatic system beneath Mount Vesuvius was initiated. A two-dimensional (2D) seismic experiment was implemented to determine the feasibility of a three-dimensional (3D) tomography of the volcano, which is located in a densely populated and noisy area.

Mount Vesuvius is a strato-volcano consisting of a volcanic cone (Gran Cono) that was built within a summit caldera (Mount Somma). The Somma-Vesuvius complex has formed over the last 25,000 years by means of a sequence of eruptions of variable explosiveness, ranging from the quiet lava outpourings that characterized much of the

latest activity (for example, from 1881 to 1899 and from 1926 to 1930) to the explosive Plinian eruptions, including the one that destroyed Pompeii and killed thousands of people in 79 A.D. At least seven Plinian eruptions have been identified in the eruptive history of Somma-Vesuvius (1). Each was preceded by a long period of quiescence, which in the case of the 79 A.D. eruption lasted about 700 years. These eruptions were fed by viscous water-rich phonolitic to tephritic phonolitic magmas that appear to have differentiated in shallow crustal conditions. They are believed to have gradually filled a reservoir where differentiation was driven by compositional convection. A minimum depth of about 3 km was inferred for the top of the magmatic reservoir from mineral equilibria of metamorphic carbonate ejecta (2). Fluid inclusions (CO_2 and $\text{H}_2\text{O}-\text{CO}_2$) in clinopyroxenes from cumulate and nodules indicate a trapping pressure of 1.0 to 2.5 kbar at about 1200°C , suggesting that these minerals crystallized at depths of 4 to 10 km (3). The differentiated magma fraction was about 30% of the total magma in the reservoir, and a volume of about 2 to 3 km^3 was inferred for the reservoir (4). The magma ascent to the surface occurred through a conduit of possibly 70 to 100 m in diameter (5). A thermal model predicts that such a

reservoir should contain a core of partially molten magma (6) that can be detected by high-resolution seismic tomography.

The most recent activity at Mount Vesuvius (1631 to 1944) was fed by tephritic phonolitic magma filling the conduit. There is no evidence of long residence times of magma in a crustal reservoir at depths greater than 1 km. Eruptive episodes appear to have been triggered by the arrival of new batches of isotopically distinct magma from greater depths that mixed with the magma in the conduit (7). Hence, the petrological evidence indicates a complicated feeding system for Mount Vesuvius in spite of the fact that most of the eruptions occur at the summit and only occasionally occur from lateral vents, which are mostly located along the southern slope of the mountain.

Little is known about shallow crustal structure beneath the volcano. A seismic reflection survey carried out in 1973 in the Bay of Naples identified a west-northwest deepening strong reflector that was interpreted as the top of the Mesozoic carbonate platform underlying the volcano (8). Deep drilling carried out for geothermal purposes on the southern slope of the volcano (Trecase well) reached the Mesozoic carbonate basement at a depth of about 1.885 km [1.665 km below sea level (bsl)] (9). Bouguer gravity anomalies were calibrated with these data and were used to model the deepening of the basement down to about 2.3 km bsl underneath the western edge of the volcano (10). The P waves reflected by the Mohorovičić discontinuity (Moho) (PmP waves) detected by a Deep Seismic Soundings experiment in the Bay of Naples suggest that the crust under Mount Vesuvius is about 35 km thick (11).

We recorded a 30-km-long northwest-trending seismic profile passing through the center of Mount Vesuvius (Fig. 1). Seismic energy was generated by blasting 340 to 410 kg of explosive at sites S1, S2, and S3, and the signals were recorded at 82 receivers deployed along the profile (12). The shot data from S2 and S3 were combined with

- A. Zollo, P. Gasparini, P. dell'Aversana, G. Iannaccone, Dipartimento di Geofisica e Vulcanologia, Università di Napoli "Federico II," Largo S. Marcellino 10, 80138, Napoli, Italy.
- J. Virieux, Institut de Geodynamique, CNRS Sophia-Antipolis, France.
- H. le Meur and R. de Matteis, Dipartimento di Geofisica e Vulcanologia, Università di Napoli "Federico II," Largo S. Marcellino 10, 80138, and Osservatorio Vesuviano, Napoli, Italy.
- G. de Natale, P. Capuano, G. Vilardo, Osservatorio Vesuviano, Napoli, Italy.
- G. Biella and R. de Franco, Istituto per le Ricerche sul Rischio Sismico, Consiglio Nazionale delle Ricerche (CNR), Milano, Italy.
- E. Boschi, Istituto Nazionale di Geofisica, Roma, Italy.
- I. Guerra, Dipartimento di Scienze della Terra, Università della Calabria, Cosenza, Italy.
- L. Mirabile, Istituto di Oceanologia, Istituto Universitario Navale, Napoli, Italy.

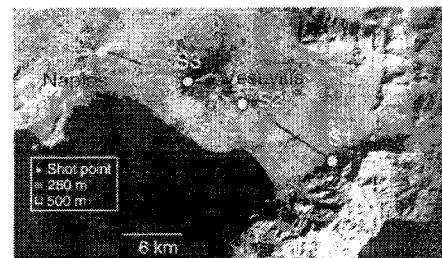


Fig. 1. Satellite image of the Vesuvius area. The shot points and the recording profile for the 1994 active seismic experiment are indicated. Colored segments of the profile are related to different receiver spacing (red = 250 m; blue = 500 m).